LA-UR -82-2644

Conf-820942--19

Los Alamos National Laboratory is operated by the University of California for the United States Department of Energy under contract W-7405-ENG-36

LA-UR--82-2644

DE83 000663

MASTER

TITLE CHARGED-PARTICLE ELASTIC CROSS SECTIONS

AUTHOR(S). G. M. Hale, T-2
D. C. Dodder, T-2
J. C. DeVenus, Univ. of Ill., Urbana, Ill.

SUBMITTED TO The Nuclear Data for Science and Technology International Conference, Antwerp, Belgium, 6-10 September 1982.

DISCLAIMER

Los Alamos Los Alamos National Laboratory
Los Alamos, New Mexico 87545

FORM NO 836 R4
ST NO 2629 5/81

DISTRIBUTION OF THIS DOCUMENT IS UNLIMITED

CHARGED-PARTICLE ELASTIC CROSS SECTIONS

G. M. Hale and D. C. Dodder

Theoretical Division, Los Alamos National Laboratory
Los Alamos, New Mexico 87545 USA

J. C. DeVeaux

214 Nuclear Engineering Laboratory
University of Illinois
Urbana, Illinois 61801 USA

Modern treatments of energy loss in plasmas through elastic scattering of energetic ions require complete knowledge of charged-particle elastic cross sections. R-matrix theory provides an explicit separation of nuclear and Coulomb effects in these cross sections, and gives reasonable extrapolations to small angles and low energies, where data may be scarce. We outline the calculation of charged-particle elastic cross sections from R-matrix parameters, and give examples for d-T, d-α, and t-α scattering, obtained from comprehensive analyses of reactions in the ^{5}He, ^{6}Li, and ^{7}Li compound systems. Expansion coefficients for an exact polynomial representation for the difference of the scattering and Rutherford cross sections (σ_{NI}) are given for d-T scattering. Integral quantities involving σ_{NI} calculated from the present cross sections disagree substantially in some cases near resonances with a recent Livermore evaluation.

[Charged-particle elastic cross sections calculated from R-matrix theory. d-T, d-α, t-α scattering at energies below 5 MeV. Polynomial representation and integrals for σ_{NI}]

Introduction

Charged-particle elastic (CPE) scattering is an important energy-loss mechanism in ionized plasmas. Traditionally, the slowing-down treatment has taken into account only the effects of Rutherford (or "pure Coulomb") scattering, in which the energy loss comes from summing over large numbers of small-angle deflections. This approximation is valid in most cases at low energies, where the Coulomb amplitude dominates the nuclear amplitudes. However, at higher energies, where energy losses are more substantial, nuclear amplitudes affect the large-angle cross sections significantly, and enter even at small angles through interference with the Coulomb amplitude. It is important, therefore, to have a method for describing all the components of CPE cross sections, which provides reasonable extrapolations to regions not accessible to measurements (usually small angles and low energies).

R-matrix theory[1] is highly suitable for such a description, since, as has been pointed out at previous Cross Section meetings[2-4], it allows a parametric treatment of short-ranged (nuclear) effects, while accounting exactly for long-ranged effects, such as the Coulomb and angular momentum barriers. Thus, the relationship between the Coulomb and nuclear parts of the cross section as a function of energy and angle is constrained by a theory that embodies the fundamental properties of nuclear interactions and ensures the correct limiting behavior at small angles and low energies, where the long-ranged effects dominate.

In the following section, we outline the calculation of CPE cross sections from R-matrix parameters, then show for a few important cases how these calculated cross sections behave as functions of energy and angle and how they compare with experimental data. In Section III, we develop an exact polynomial representation for the difference of the CPE and Rutherford cross sections (σ_{NI}), and illustrate the behavior of this cross section and some of its expansion coefficients. Applications involving integrals of σ_{NI} are discussed in Section IV, where results based on the present R-matrix cross sections are compared with another recent evaluation. The final section summarizes the important points of the previous discussion and gives conclusions.

R-matrix Description of CPE Scattering

Elements of the R matrix are given by projections of essentially the Green's function operator for the internal Hamiltonian of a system of interacting particles on the two-body channel surface of the system[2]. They can be expressed as

$$R_{c'c} = \sum_\lambda \frac{\gamma_{c'\lambda}\gamma_{c\lambda}}{E_\lambda - E} \quad , \tag{1}$$

where the $\gamma_{c\lambda}$ and E_λ are reduced-width amplitudes and eigenenergies, respectively, for states $|\lambda\rangle$ having logarithmic derivative projections B_c on the channel surface defined by radii $r_c = a_c$. The channel label $|c\rangle = |\alpha J s \ell\rangle$ denotes a 2-body arrangement α of the system of particles having quantum numbers J, s, ℓ associated with total angular momentum, total spin, and orbital angular momentum, respectively.

In order to calculate observables, such as cross sections, of a scattering process, it is necessary to have matrix elements of the transition operator. These are related to the R matrix by[2,5]

$$T_{c'c} = e^{i\omega_{c'}} P_{c'}^{1/2} [R^{-1}-(L-B)]^{-1}_{c'c} P_c^{1/2} e^{i\omega_c}$$

$$- e^{2i(\omega_c - \phi_c)} \delta_{c'c} \tag{2}$$

where B is the diagonal matrix of boundary-condition numbers B_c and L is a diagonal matrix containing logarithmic derivatives of channel outgoing spherical Coulomb waves, which can be expressed as

$$L_c = S_c + iP_c \quad , \tag{3}$$

in terms of the channel shift and penetrability functions, S_c and P_c. The quantities ω_c and $-\phi_c$ are phase shifts for Coulomb and hard-sphere scattering, respectively. Note that because of the matrix inversions in (2), any element of T depends, in general, on all the elements of R, and vice versa.

Observables for elastic scattering involve only the T-matrix elements for which $\alpha' = \alpha$. If these are denoted by

$$T_{c'c}(\alpha' = \alpha) = t^J_{s'\ell', s\ell} \quad ,$$

then the elastic scattering cross section for charged particles can be written as the sum of three terms:

$$\sigma(\mu) = \sigma_R(\mu) + \sigma_N(\mu) + \sigma_I(\mu) \quad , \tag{6}$$

where for $\mu = \cos(\theta_{CM})$, the "pure Coulomb," or Rutherford scattering cross section is

$$\sigma_R(\mu) = \left[\frac{\eta}{k(1-\mu)}\right]^2 \quad , \tag{5}$$

the "pure nuclear" cross section is

$$\sigma_N(\mu) = [(2s_1+1)(2s_2+1)k^2]^{-1} \sum_L \sum_{s's} (-1)^{s'-s} \sum_{J_1 J_2 \ell_1' \ell_2' \ell_1 \ell_2} \bar{Z}(\ell_1' J_1 \ell_2' J_2, s'L) \; \bar{Z}(\ell_1 J_1 \ell_2 J_2 sL)$$
$$\mathrm{Re}(t^{J_1}_{s'\ell_1',s\ell_1} t^{J_2 *}_{s'\ell_2',s\ell_2}) \; P_L(\mu) \tag{6}$$

and the Coulomb-nuclear interference cross section is

$$\sigma_I(\mu) = - \frac{2\eta}{(2s_1+1)(2s_2+1)k^2(1-\mu)} \quad \mathrm{Re}[e^{i\eta \ell n \frac{1}{2}(1-\mu)}$$
$$\sum_{Js\ell} \quad (2J+1) t^J_{s\ell,s\ell} \; P_\ell(\mu)] \quad . \tag{7}$$

in Eqs. (5)-(7), k is the center-of-mass wave number and η the Coulomb parameter for a distinguishable pair of interacting particles, s_1 and s_2 are their spins, $\bar{Z}$ is a modified Racah coefficient as defined in Ref. 5, and $P_n(\mu)$ is the n^{th} order Legendre polynomial.

Elastic scattering cross sections calculated from relations (4)-(7) are shown in Figs. 1-3 for the case of d-T, d-α, and t-α scattering. These are the primary cross sections that are required when considering the slowing down of fast ions in a d-T plasma. The R-matrix parameters used in these calculations came from comprehensive studies of reactions in the ^{5}He, ^{6}Li, and ^{7}Li systems, some of which have been described in Refs. 2 and 3. The term "comprehensive" implies that many measurements for other reactions and observables were included in the analyses along with elastic scattering cross section data. Data for other reactions influence the elastic T-matrix elements through the relation between R and T noted above in connection with Eq. (2).

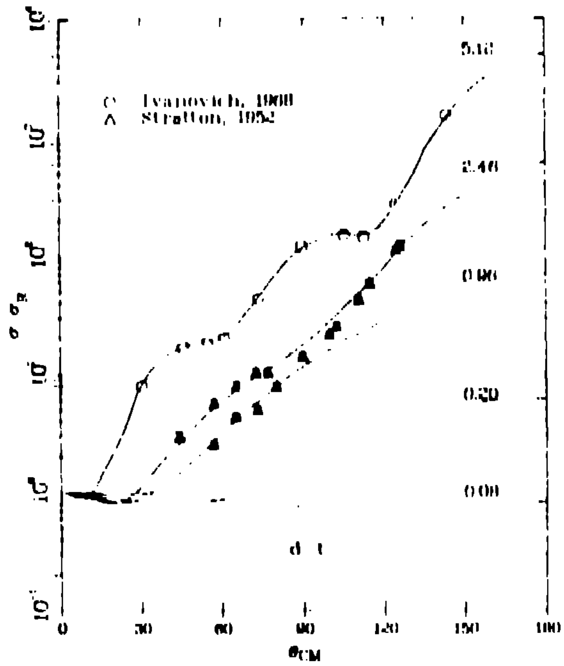

Fig. 1. Calculated and measured cross-section ratios to Rutherford scattering for d-T. The data (▲) at .96 and 2.46 MeV are those of Stratton[6]; those (○) at 5.18 MeV are from Ivanovich[7].

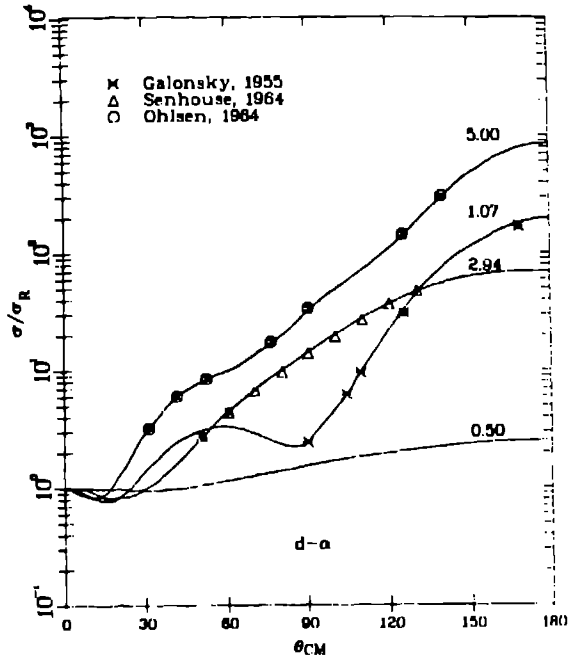

Fig. 2. Calculated and measured cross-section ratios to Rutherford scattering for d-α. The data at 1.07 MeV are those of Galonsky[8]; those at 2.94 MeV are from Senhouse[9]; those at 5.00 MeV are from Ohlsen[10].

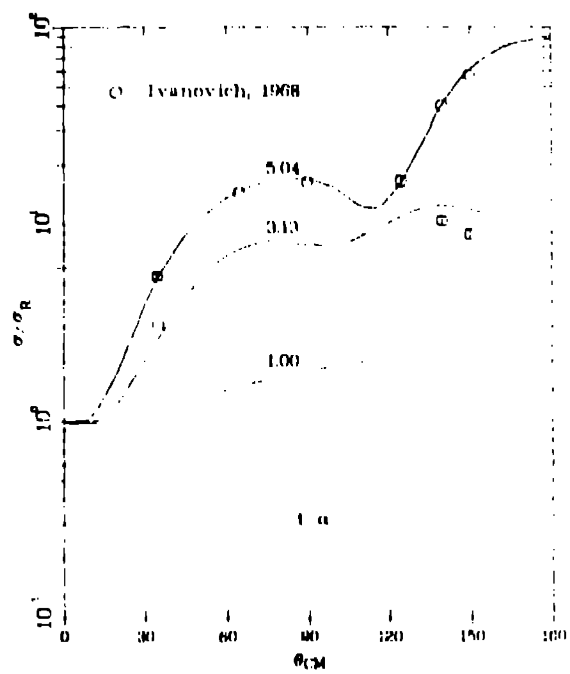

Fig. 3. Calculated and measured cross-section ratios to Rutherford scattering for t-α. The data at 3.13 and 5.04 MeV are those of Ivanovich[7].

The scattering cross sections in Figs. 1-3 are plotted as ratios to the Rutherford cross section, so that the effect of the nuclear amplitudes can easily be seen as deviations from unity. The onset of significant deviations from pure Coulomb scattering occurs at fairly low energies for all three reactions, but especially for d-T (Fig. 1). This is due mainly to the presence of prominent resonances in the reactions: a relatively broad $3/2^+$ resonance in d-T at $E_d \approx 200$ keV (109 keV in the T(d,n)α reaction), a narrow 1^+ resonance in d-α at $E_d = 1.07$ MeV, and a relatively narrow $7/2^-$ resonance in t-α at $E_t = 1.85$ MeV. In all three cases, the calculations indicate substantial deviations from pure Coulomb scattering at energies below the lowest energy where measurements have been made.

Fig. 1 shows predictions for d-T at 80 and 200 keV, then comparisons with the data of Stratton[6] at .96 MeV (the lowest energy measurements) and 2.46 MeV, and with those of Ivanovich[7] at 5.18 MeV. The agreement of the calculation with the data is fair at the lower two energies and good at the upper energy. The $3/2^+$ resonance gives strong contributions from the interference cross sections in the calculations for d-T, causing the interference minimum that diminishes and moves to smaller angles as the energy increases. The interference is so strong at 80 keV, however, that the scattering cross section falls below the Rutherford cross section at all angles greater than 30°.

Fig. 2 shows predictions for d-α at 500 keV and comparisons with the data of Galonsky[8] at 1.07 MeV, of Senhouse[9] at 2.94 MeV, and of Ohlsen[10] at 5.00 MeV. There is good agreement between the calculations and the measurements in this energy range. The D-wave resonance at 1.07 MeV causes more structure in the angular distribution and a deeper interference minimum at this energy than at nearby energies.

Fig. 3 shows predictions for t-α at 1 MeV and comparisons with measurements of Ivanovich[7] at 3.13 and 5.04 MeV. The agreement between the calculation and the data is poor at 3.13 MeV and good at 5.04 MeV. In this case, the energy of the resonance is relatively high, so that deviations from pure Coulomb scattering are less dramatic at low energies than for the other two reactions.

Exact Polynomial Representation for σ_{NI}

From Eqs. (5)-(7), it can be seen that the sum of the nuclear and interference cross sections,

$$\sigma_{NI}(\mu) = \sigma_N(\mu) + \sigma_I(\mu) \quad ,$$

can be expanded in Legendre polynomials, according to

$$\sigma_{NI}(\mu) = -\frac{2\eta}{1-\mu}\,\mathrm{Re}\Big[e^{i\eta\ln\frac{1}{2}(1-\mu)}\sum_{\ell=0}^{\ell mx}\frac{2\ell+1}{2}\,a_\ell P_\ell(\mu)\Big] + \sum_{\ell=0}^{2\ell mx}\frac{2\ell+1}{2}\,b_\ell P_\ell(\mu) \quad , \tag{8}$$

with

$$\frac{2\ell+1}{2}\,a_\ell = [(2s_1+1)(2s_2+1)k^2]^{-1}\sum_{Js}(2J+1)\,t^J_{s\ell,s\ell} \tag{9}$$

and

$$\frac{2\ell+1}{2}\,b_\ell = [(2s_1+1)(2s_2+1)k^2]^{-1}\sum_{s's}(-1)^{s'-s}$$

$$\sum_{J_1J_2\ell'_1\ell'_2\ell_1\ell_2}\bar{Z}(\ell'_1J_1\ell'_2J_2,s'\ell)\,\bar{Z}(\ell_1J_1\ell_2J_2,s\ell)$$

$$\mathrm{Re}\big(t^{J_1}_{s'\ell'_1,s\ell_1}\,t^{J_2*}_{s'\ell'_2,s\ell_2}\big) \quad . \tag{10}$$

The sums in Eqs. (8)-(10) are limited by neglecting partial waves for nuclear scattering above ℓmx. As can be seen from Eqs. (9) and (10), the coefficients a_ℓ are complex (as are the t's), the b_ℓ are real, and the two sets are not independent. Therefore, it is not possible to fit experimental data directly in terms of a_ℓ and b_ℓ coefficients treated as independent parameters. An intermediate step, such as an R-matrix or phase-shift analysis, is necessary to establish the relation among the a's and b's ...

The exact polynomial expansion described above is one option allowed for representing elastic scattering cross sections in a new ENDF charged-particle format[11]. The format simply specifies a tabulation of the a_ℓ and b_ℓ coefficients as a function of energy. Files of the coefficients calculated from R-matrix parameters are available at Los Alamos National Laboratory for the reactions and energy ranges listed in Table I. From these coefficients, elastic scattering cross sections can be constructed over the entire angular range for most of the reactions among light charged particles from protons through alpha particles.

Table I Charged-Particle Elastic Cross Sections Available from Los Alamos R-matrix Analyses

Mat #	Reaction	Energy Range (MeV)
2002	p-p	0-20
2004	p-T	0-11
2005	p-^{3}He	0-10
2006	p-^{4}He	0-20
3003	d-d	0-10
3004	d-T	0-8
3005	d-^{3}He	0-8
3006	d-^{4}He	0-10
4004	t-t	0-3.5
4006	t-^{4}He	0-14
5006	^{3}He-^{4}He	0-12

The behavior of the expansion coefficients a_ℓ and b_ℓ as a function of energy is illustrated in Figs. 4 and 5 for d-T scattering. Fig. 4 shows the important b_ℓ coefficients for expanding the nuclear cross section at energies below 5 MeV. The low-energy d-T S-wave resonance is clearly evident as a peak in the b_0 coefficient at 200 keV. The real and imaginary parts of the a_ℓ coefficients are shown in Fig. 5, where again, the effect of the S-wave resonance is seen at low energies in a_0.

The separation of CPE cross sections into components given by R-matrix calculations allows one to see an interesting feature not normally visible in experimental data: the rapid oscillations at small angles

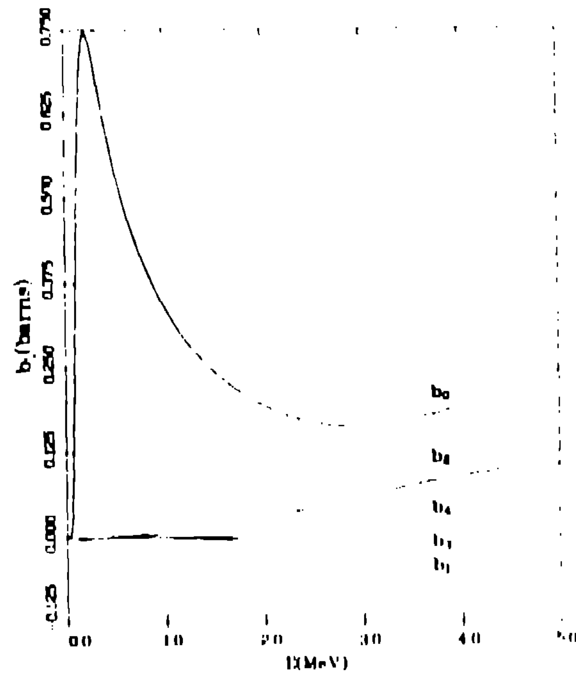

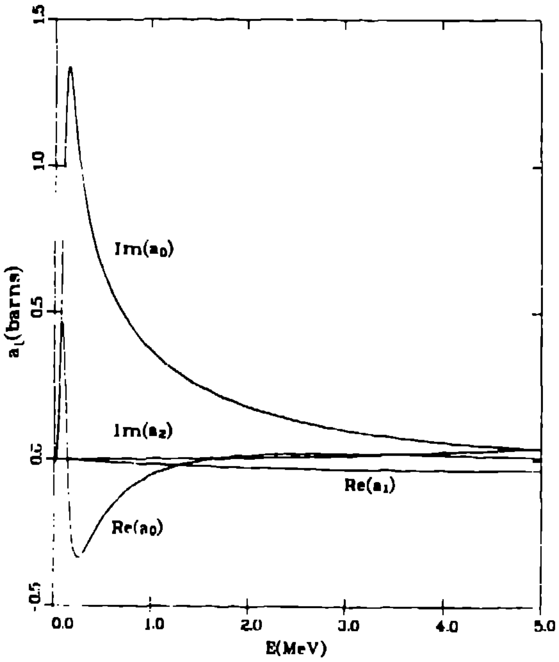

Fig. 5. Significant a_ℓ coefficients for d-T scattering at energies below 5 MeV.

in the interference cross section that are masked by the Rutherford cross section. These are illustrated in Fig. 6 by plotting $(1-\mu)\sigma_{NI}(\mu)$ for d-T scattering at 200 keV (Multiplying $\sigma_{NI}(\mu)$ by $(1-\mu)$ removes the pole at $\mu = 1$ in $\sigma_I(\mu)$; see Eq. 7.) Such oscillations are important in practice only at angles for which $\sigma(\mu) \neq \sigma_R(\mu)$ (in this case, $\theta_{CM} > 5°$), where they sometimes appear in the data as "Coulomb-nuclear interference" minima, but they introduce the mathematical difficulty that integrals of $\sigma_{NI}(\mu)$ over the entire angular range are undefined. We will return to this point in the next section.

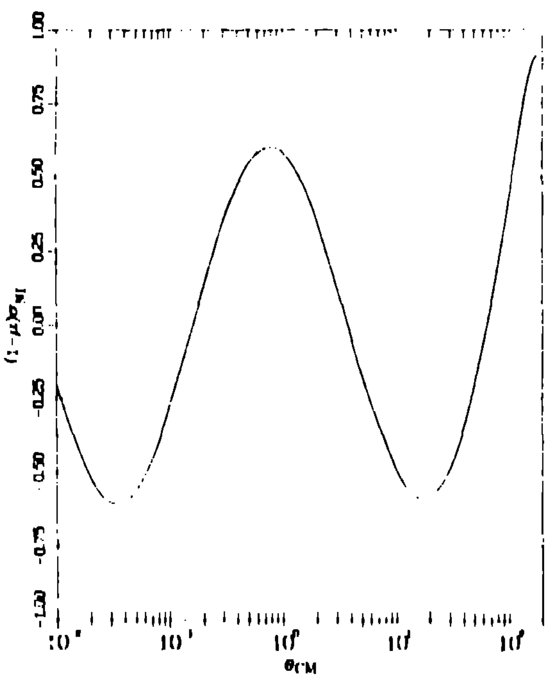

Fig. 6. Oscillatory behavior of $(1-\mu)\sigma_{NI}(\mu)$ for d-T scattering at 200 keV.

Integrals of σ_{NI}

In many CPE energy-loss calculations, the Rutherford cross section is treated with a continuous slowing-down model, while the remainder of the cross section, $\sigma_{NI}(\mu)$, is used in a discrete-event, Monte-Carlo transport framework. In such applications, integrals of $\sigma_{NI}(\mu)$ with other functions of μ are required, in principle, over the entire angular range. If σ_{NI} is to have the physical significance of a cross section, its integral over all angles must exist and be positive definite. The nuclear part of σ_{NI} satisfies these conditions, with $\sigma_N(\text{int.}) = 2\pi b_0$; but, as was mentioned at the end of the last section, the integral of σ_I over all angles is undefined due to divergent oscillations as $\mu \to 1$. Therefore, it is necessary to introduce a small-angle cutoff into the integrals of $\sigma_{NI}(\mu)$ in order to define a value for the integrated cross section, which in conventional useage should be positive.

For these reasons, integrals of σ_{NI} defined by Perkins and Cullen[12] are cut off at $\theta_{CM} = 20°$ (μ=.94), or at the largest angle (if > 20°) where σ_{NI} crosses through zero and remains positive. For the d-T cross section shown in Fig. 6, the cutoff angle according to their prescription would be 66°. Such an integral for d-T at 80 keV presumably would be zero, since σ_{NI} remains negative at angles out to 180°. In all cases, this prescription neglects the "interference" region of the cross section, where $\sigma/\sigma_R = 1 + \sigma_{NI}/\sigma_R < 1$.

However, in order to compare with the work of Ref. 12, we have calculated from our R-matrix cross sections the following integrals for $\sigma_{NI}(\mu)$:

$$\text{Integrated cross section} = \sigma_{NI}(\text{int.}) = 2\pi \int_{-1}^{\mu_c} \sigma_{NI}(\mu)d\mu$$

$$\text{Reaction rate} = \langle\sigma v\rangle = 2\pi \int_{-1}^{\mu_c} v_{rel}\sigma_{NI}(\mu)d\mu$$

$$= v_{rel}\sigma_{NI}(\text{int.}),$$

$$\text{Frac. energy loss/collision} = \left\langle\frac{\Delta E}{E}\right\rangle = \frac{4\pi m_1 m_2}{(m_1+m_2)^2}$$

$$\frac{1}{\sigma_{NI}(\text{int.})} \int_{-1}^{\mu_c} (1-\mu)\, \sigma_{NI}(\mu)\, d\mu,$$

$$\text{Frac. energy loss/unit path length} = \left\langle\frac{\Delta E}{E}\right\rangle \sigma_{NI}(\text{int.}),$$

Ave. Lab. Scatt. Cosine

$$\langle\mu_{Lab}\rangle = \frac{2\pi}{\sigma_{NI}(\text{int.})} \int_{-1}^{\mu_c} \frac{m_1+m_2\mu}{\sqrt{m_1^2+2m_1m_2\mu+m_2^2}}\, \sigma_{NI}(\mu)d\mu,$$

with the cutoff $\mu_c = \min(.94, \mu_0)$, $\sigma_{NI}(\mu_0) = 0$. The last four quantities are plotted for d-T scattering as dashed curves in Fig. 7, compared to solid curves representing the evaluation of Perkins and Cullen[12]. The agreement is fairly good at energies above 2 MeV, but there are substantial differences at low energies in the region of the S-wave resonance, where our calculations give much larger reaction rates and energy losses. This trend is also evident in comparisons for other reactions where the differences are not quite as large, but largest near the resonances.

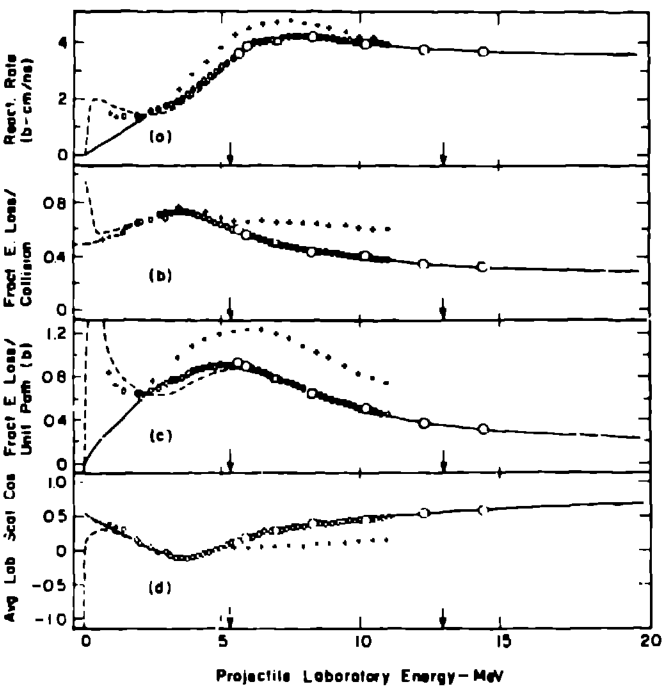

Fig. 7. Integrals of σ_{NI} for d-T scattering, as described in the text. The dashed curves are from the present calculations, the solid curves are evaluations of Perkins and Cullen[12], and the symbols represent measurements.

Summary and Conclusions

Calculating CPE cross sections from R-matrix parameters allows the separation of σ_{NI} into its constituent nuclear and Coulomb-nuclear-interference parts. The nuclear part has a well-behaved Legendre expansion with properties identical to those used to represent neutron cross sections. The interference part also has a Legendre expansion, but exhibits diverging, increasingly rapid oscillations as $\mu \to 1$. In practice, these oscillations are important only at angles for which σ_{NI}/σ_R differs noticeably from zero, where they cause measureable "interference minima" in the cross sections.

Coefficients for the Legendre expansion of σ_{NI}, tabulated vs energy in a new ENDF format, are available for most of the reactions involving protons through ^{4}He. These coefficients are calculated from R-matrix parameters resulting from comprehensive studies of few-nucleon systems done at Los Alamos over the past several years. The R-matrix calculations generally agree well with existing cross-section measurements, and provide reliable extrapolations to energies and angles where measurements are not available.

For the important case of d-T scattering, for instance, cross-section measurements do not extend to energies low enough to see the major effects of the strong 3/2 S-wave resonance. These effects are clearly evident in the low-energy calculations, however, as peaks in the a_ℓ and b_ℓ expansion coefficients, strong interference terms in the cross section, and pronounced deviations from Rutherford scattering at backward angles. The effects of the resonance are also responsible for large differences at low energies between calculated integrals of σ_{NI} and a recent evaluation of Perkins and Cullen.

The oscillatory behavior of σ_I at small angles prevents defining an integrated cross section for σ_{NI} without introducing a small-angle cutoff. If the cutoff is chosen so that σ_{NI}(int.) is positive definite, as is required by its use in some slowing-down interference region are neglected. These difficulties suggest that an improved method of dealing with CPE cross sections in slowing-down calculations is required. One possibility is to apply the continuous slowing-down treatment to the sum of the Rutherford and interference cross sections, leaving the well-behaved nuclear cross section to be used in Monte-Carlo transport. Another is to use the present (σ_R, σ_{NI}) separation, but place the cutoff angle where σ begins to deviate from σ_R. This prescription does not guarantee a positive-definite integrated cross section for σ_{NI}, however, and would require physical interpretation in the Monte-Carlo transport of a cross section that is sometimes negative with respect to Rutherford scattering.

The present calculations provide the separation and detail necessary to be useful, regardless of the methods finally chosen to apply charged-particle elastic cross sections to the important problems of fusion energy design.

References

1. E. P. Wigner and L. Eisenbud, Phys. Rev. 72, 29 (1974).

2. G. M. Hale and D. C. Dodder, Proc. Conf. Nuclear Cross Sections for Technology, Knoxville 1979 (NBS Spec. Pub. 594), p. 650 (1980).

3. G. M. Hale, Proc. Symp. Neutron Standards and Applications, Gaithersburg, 1977 (NBS Special Pub. 493), p. 30 (1977).

4. G. M. Hale, Proc. Conf. Nuclear Data Evaluation Methods and Procedures, Brookhaven 1980 (BNL-NCS-51363, Vol. II), p. 509 (1981).

5. A. M. Lane and R. G. Thomas, Rev. Mod. Phys. 30, 257 (1958).

6. W. R. Stratton, G. D. Freier, G. R. Keepin, P. Rankin, and T. F. Stratton, Phys. Rev. 88, 257 (1952).

7. M. Ivanovich, P. G. Young, and G. G. Ohlsen, Nucl. Phys. A110, 441 (1968).

8. A. Galonsky, R. A. Douglas, W. Haeberli, M. T. McEllistrem, and H. T. Richards, Phys. Rev. 98, 586 (1955).

9. L. S. Senhouse and T. A. Tombrello, Nucl. Phys. 57, 624 (1964).

10. G. G. Ohlsen and P. G. Young, Nucl. Phys. 52, 134 (1964).

11. R. E. MacFarlane, G. M. Hale, and P. G. Young, "Charged Particle Format," ENDF draft report (1981).

12. S. T. Perkins and D. E. Cullen, Nucl. Sci. Eng. 77, 20 (1981).